OFFICE OF NAVAL RESEARCH

Research Contract N00014-91-J-1909

R&T Code 4133035

Program Manager Robert J. Nowak

Technical Report No. 6

"Hydrogen Bonding and Surface Interactions among Protic Solvents: Coadsorption of Ammonia and Hydrogen Fluoride with Water on Silver(110)"

by

A. Krasnopoler, N. Kizhakevariam, and E. M. Stuve

Prepared for Publication

in

Journal of the Chemical Society, Faraday Transactions

University of Washington
Department of Chemical Engineering
Box 351750
Seattle, WA 98195-1750

August, 1995

Reproduction in whole, or in part, is permitted for any purpose of the United States Government.

This document has been approved for public release and sale; its distribution is unlimited.

19950822 031

REPORT DOCUMENTATION PAGE

Form Approved
OMB No. 0704-0188

Public reporting burden for this collection of information is estimated to average 1 hour per response, including the time for reviewing instructions, searching existing data sources, gathering and maintaining the data needed, and completing and reviewing the collection of information. Send comments regarding this burden estimate or any other aspect of this collection of information, including suggestions for reducing this burden to Washington Headquarters Services, Directorate for Information Operations and Reports, 1215 Jefferson Davis Highway, Suite 1204, Arlington, VA 22202-4302, and to the Office of Management and Budget, Paperwork Reduction Project (0704-0188), Washington, DC 20503.

1. AGENCY USE ONLY *(Leave Blank)*	2. REPORT DATE	3. REPORT TYPE AND DATES COVERED
	15 August 1995	6/95 – 5/96

4. TITLE AND SUBTITLE

Hydrogen Bonding and Surface Interactions among Protic Solvents: Coadsorption of Ammonia and Hydrogen Fluoride with Water on Silver(110)

5. FUNDING NUMBERS

N00014-91-J-1909

R&T Code 4133035

Robert J. Nowak

6. AUTHOR(S)

A. Krasnopoler, N. Kizhakevariam, and E. M. Stuve

7. PERFORMING ORGANIZATION NAME(S) AND ADDRESS(ES)

University of Washington
Department of Chemical Engineering
Box 351750
Seattle, WA 98195-1750

8. PERFORMING ORGANIZATION REPORT NUMBER

Technical Report No. 6

9. SPONSORING / MONITORING AGENCY NAME(S) AND ADDRESS(ES)

Office of Naval Research
800 N. Quincy Street
Arlington, VA 22217

10. SPONSORING/MONITORING AGENCY REPORT NUMBER

DTIC ELECTE AUG 23 1995 B

11. SUPPLEMENTARY NOTES

12a. DISTRIBUTION / AVAILABILITY STATEMENT

This document has been approved for public release and sale; its distribution is unlimited.

12b. DISTRIBUTION CODE

DTIC QUALITY INSPECTED 8

13. ABSTRACT *(Maximum 200 words)*

Coadsorption of water with either ammonia or hydrogen fluoride on a Ag(110) substrate was studied to examine the relationships between intermolecular hydrogen bonding near the surface and preferential adsorption at the surface. The experiments were conducted in ultrahigh vacuum with facilities for thermal desorption spectroscopy and high resolution electron energy loss spectroscopy. Adsorption was performed at 110 K for ammonia and water and at 90 K for hydrogen fluoride and water. Ammonia and water simply coadsorb at 110 K with no evidence of specific hydrated complexes nor of ionization to NH_4^+. Coadsorbed water enhances population of the chemisorbed state of ammonia, which we estimate to have a saturation coverage of 0.12 monolayer without water, through a mechanism of dielectric screening. At coverages approaching one monolayer and higher, water stabilizes the bulk of ammonia, increasing the average desorption temperature by as much as 21 K from 134 K. Stabilization energies estimated from these temperature shifts range from 2 to 5 kJ/mol NH_3 and from 1 to 9 kJ/mol H_2O. In contrast, hydrogen fluoride and water form a well defined monohydrate $HF{\cdot}H_2O$, as evidenced by the coincident thermal desorption curves of both species. The monohydrate behaves as an adlayer azeotrope and thermal desorption measurements can be used to follow the sublimation temperature as a function of adlayer composition. From these data so-called bubble-point and dew-point curves can be developed by analogy with normal binary solutions.

14. SUBJECT TERMS

Ammonia Adsorption, Water Adsorption, Solvation, Hydrogen Bonding Hydrogen Fluoride Adsorption, Adsorbate Thermodynamics, Silver(110), Metal/Electrolyte Interface

15. NUMBER OF PAGES

36

16. PRICE CODE

17. SECURITY CLASSIFICATION OF REPORT	18. SECURITY CLASSIFICATION OF THIS PAGE	19. SECURITY CLASSIFICATION OF ABSTRACT	20. LIMITATION OF ABSTRACT
Unclassified	Unclassified	Unclassified	

Hydrogen Bonding and Surface Interactions among Protic Solvents: Coadsorption of Ammonia and Hydrogen Fluoride with Water on Silver(110)

A. Krasnopoler, N. Kizhakevariam, and E. M. Stuve*

University of Washington

Department of Chemical Engineering

Box 351750

Seattle, Washington 98195-1750 USA

Submitted to:

Journal of the Chemical Society, Faraday Transactions

July, 1995

Accession For
NTIS GRA&I ☑
DTIC TAB ☐
Unannounced ☐
Justification
By
Distribution
Availability Codes
Dist | Avail and/or Special
A-1

*Address correspondence to this author.

E-mail: Stuve@u.washington.edu; Fax: +206.543.3778.

ABSTRACT

Coadsorption of water with either ammonia or hydrogen fluoride on a Ag(110) substrate was studied to examine the relationships between intermolecular hydrogen bonding near the surface and preferential adsorption at the surface. The experiments were conducted in ultrahigh vacuum with facilities for thermal desorption spectroscopy and high resolution electron energy loss spectroscopy. Adsorption was performed at 110 K for ammonia and water and at 90 K for hydrogen fluoride and water. Ammonia and water simply coadsorb at 110 K with no evidence of specific hydrated complexes nor of ionization to NH_4^+. Coadsorbed water enhances population of the chemisorbed state of ammonia, which we estimate to have a saturation coverage of 0.12 monolayer without water, through a mechanism of dielectric screening. At coverages approaching one monolayer and higher, water stabilizes the bulk of ammonia, increasing the average desorption temperature by as much as 21 K from 134 K. Stabilization energies estimated from these temperature shifts range from 2 to 5 kJ/mol NH_3 and from 1 to 9 kJ/mol H_2O. In contrast, hydrogen fluoride and water form a well defined monohydrate $HF{\cdot}H_2O$, as evidenced by the coincident thermal desorption curves of both species. The monohydrate behaves as an adlayer azeotrope and thermal desorption measurements can be used to follow the sublimation temperature as a function of adlayer composition. From these data so-called bubble-point and dew-point curves can be developed by analogy with normal binary solutions.

1. INTRODUCTION

The nature of hydrogen bonding in metal/solvent interactions is of primary importance in electrochemical and corrosion processes. Interactions with the substrate disrupt the normal hydrogen bonded structure of protic solvents and a competition develops between solvent molecules interacting with themselves and preferential adsorption at the surface. Additional complications arise when hydrogen bonding exists with other species of importance. For example, the initial scission of the C–H bond in methanol electrocatalysis has been attributed to preferential orientation of the CH_3 group towards the surface on account of hydrogen bonding between the OH group and water [1].

To date most surface science studies of metal/solvent interactions have concentrated on water, as it is the most common solvent. Water does not preferentially adsorb on Ag(110) as seen by the single desorption peak that occurs at all coverages [2-4]. Because of this weak interaction Ag(110) is a prime candidate for studies of solvent adsorption, since the ability of coadsorbates to induce some kind of preferential adsorption can be readily monitored [4,5]. Indeed, much of our previous work in this regard can be characterized as studies of water interacting with strongly adsorbed coadsorbates like O [2,3], Cl [6], F [7,8], and ClO_4 [5,9]. In this paper, we consider water interacting with two weakly coadsorbing species, ammonia and hydrogen fluoride, that partake in hydrogen bonding interactions with themselves as well as with water, regardless of the nature of the substrate.

Ammonia adsorption has been studied on a number of surfaces, including Ag(110) [10], Ag(311) [11], Au(111) [12], Cu(100) [13], Cu(111) [14,15],

Ni(110) [16], Pt(111) [17], and Ru(0001) [18,19]. In general, three adsorption states occur for adsorption on the noble metals. Chemisorbed ammonia is the most strongly bound and is characterized by a broad desorption peak in the range of 150 to 300 K depending on the substrate. Adsorption occurs through the nitrogen atom. This state usually saturates at a low coverage and exhibits repulsive interactions. Second layer ammonia, which is hydrogen bonded to the chemisorbed layer, is the next most strongly bound; desorption temperatures of 120 to 200 K are common for this state. Multilayer ammonia is the most weakly bound and desorbs in a sharp peak at 115 K under ultrahigh vacuum conditions, regardless of the substrate. To our knowledge, there have been no coadsorption studies of water and ammonia.

Thick films of ammonia monohydrate, in both amorphous and crystalline forms, have been studied by infrared spectroscopy [20-22]. The monohydrate is characterized by strong absorbances at 800 and 1100 cm^{-1} representing librational modes of water and the ν_2 (umbrella) mode of ammonia, respectively. Far infrared measurements and molecular structure calculations have also been performed [23-26]. The hydrogen bond between ammonia and water in the monohydrate has been calculated to be 25 kJ/mol [34] and the "stability" of the complex with respect to the next available state has been calculated to be 16 kJ/mol [26].

We know of only one other study of hydrogen fluoride adsorption, which also includes coadsorption with water. On Pt(111) [27] hydrogen fluoride has two adsorption states: the first layer state, which desorbs at 130 K, and the multilayer state, which desorbs at 126 K. It is interesting to note that the multilayer desorption temperatures for both ammonia and hydrogen fluoride are similar, yet the two species have quite different interactions with the

surface [5]. Hydrogen fluoride ionizes in the presence of water to form hydronium ion H_3O^+ and fluoride ion F^- on Pt(111) [27]. We discussed hydrogen fluoride/water coadsorption on Ag(110) briefly in an earlier publication [5], concentrating on the behavior at submonolayer coverages. On Ag(110), the mixed adlayer forms an azeotrope so identified by the desorption of both species at temperatures higher than for either species adsorbed alone. In this report, we focus on multilayer coverages and illustrate detection of the monohydrate $HF \cdot H_2O$ with thermal desorption measurements.

2. EXPERIMENTAL PROCEDURE

The experiments were performed in a stainless steel ultrahigh vacuum chamber, with a base pressure of 10^{-8} Pa, that has been described previously [28,29]. Details of substrate preparation and characterization have also been given previously [8]. The substrate was attached to tantalum wires and mounted onto a liquid nitrogen cooled sample holder. The tantalum wires provided resistive heating and conductive cooling of the sample.

Ammonia exposures were made through a 6.35 mm diameter stainless steel tube with a cone-shaped nozzle (45° angle, 35 mm exit diameter) mounted on the end. A diffuser made of tantalum foil was placed at the outlet of the cone. During adsorption the doser assembly was located 5 mm from the substrate. Water exposures were made through a glass capillary array doser [28] that was also brought close to the substrate during dosing.

Electron energy loss spectra were measured in specular reflection with a primary beam energy of 1.6 – 2 eV at 60° incidence from the surface normal. The typical resolution of the elastic peak (full width at half-maximum) was

100 cm^{-1}, and all energy losses are reported to the nearest 5 cm^{-1}. Spectrometer detuning at high energy losses obscured the O–H and N–H stretching regions in some of the spectra. Detuning occurs when the scattered beam does not follow a straight trajectory from substrate to analyzer. This can be compensated, without altering the spectrum, by retuning the spectrometer specifically for the high energy losses as was done in Figs. 5(b,d). A computer data acquisition scheme was used to obtain constant counting statistics for any magnification of the spectrum. The spectrometer was held at a particular energy loss and the time required to obtain 100 counts measured. The energy loss was then incremented and the process repeated. The times were converted to counting frequency as a function of energy loss and the spectra reported in the normal fashion.

Coverages of water and ammonia were determined by the integrated thermal desorption curves. The signal for water was calibrated with known standards [3,6]. Although no similar calibration methods are known for ammonia, the maximum amount of thermal desorption exclusive of the multilayer peak was used to define a saturated layer of ammonia. As discussed in the Results section, this saturated layer was assumed to have a coverage of 1.16 monolayer based on the substrate. The error in this assumption is thought to be less than 15%, and the convenience of having an approximate absolute coverage makes such an assumption appropriate. All coverages are reported in units of monolayers (ML) based on the number of topmost silver atoms (8.45×10^{14} cm^{-2}). All exposures and energy loss measurements for the ammonia/water system were performed with the sample at 110 K.

Thermal desorption measurements were performed with a Balzers QMG

112 mass spectrometer attached to a computer for multiple signal acquisition [30]. Thermal desorption of water was monitored with a mass-to-charge ratio *m/z* of 18. Ammonia desorption was monitored by *m/z* = 16 to avoid the strong overlap of OH^+ and NH_3^+ at mass 17. The signal for mass 16 was corrected for the contribution by water as follows. The ratio of H_2O^+:OH^+:O^+ for water was found to be 100:26:2.6, in agreement with previous reports [31]. The reported ammonia desorption curves I_A were then corrected from the *m/z* = 16 signal of the mass spectrometer I_{16} by digitally subtracting the contribution of water as given by the *m/z* = 18 signal I_{18},

$$I_A = I_{16} - 0.026\, I_{18}. \qquad (1)$$

The heating rate for all thermal desorption measurements was 5 K/s.

The hydrogen fluoride/water coadsorption experiments were performed with a different sample holder capable of temperatures as low as 80 K. Hydrogen fluoride was dosed through a 6.35 mm stainless steel tube with no cone or diffuser. Hydrogen fluoride coverage was calibrated by the adlayer azeotrope that forms at a 1:1 ratio with water [5].

3. RESULTS

Thermal desorption curves of pure water and ammonia are shown in Fig. 1. In agreement with earlier studies [2,3], water desorbs in a single peak at about 160 K depending on coverage; the onset of water desorption is 146 K. By contrast, ammonia has three distinct desorption features: a broad, high temperature peak extending from 140 to 190 K, a peak between 125 and 130 K, and a sharp peak at about 110 to 115 K (not shown). The broad high

temperature peak is attributed to chemisorbed ammonia [10,11], the peak at 125 to 130 K to second layer ammonia, and the sharp, low temperature peak to multilayer ammonia [10]. This last peak does not appear in these results because the adsorption temperature of 110 K prevented accumulation of ammonia multilayers.

The uptake of ammonia as a function of exposure is shown in the inset of Fig. 1; the asymptotic approach to a saturation value is consistent with the absence of a multilayer adsorption state. In order to obtain molar ratios of water to ammonia, it is necessary to have an absolute measure of ammonia coverage. Unfortunately, a suitable calibration point for ammonia is not known. An estimate of the saturation coverage may be obtained on the assumption that the second layer of ammonia has the same packing density as for solid ammonia. This assumption is equivalent to that frequently used for water, namely, that the saturated "first layer" of water is actually a perfect bilayer, the coverage of which amounts to 1.18 ML on Ag(110). Solid ammonia exists in a cubic structure and from the dimension of the cube axis, 5.1 Å at 77 K [32], the maximum packing density of ammonia of 8.88×10^{14} cm^{-2} can be found. Including the chemisorbed layer, which is 10% of the second layer (Fig. 1), the saturation coverage of ammonia is estimated to be 9.8×10^{14} cm^{-2}, or 1.16 ML on the Ag(110) basis. The error in this estimate is thought to be less than 15%. It is interesting to note that the saturation coverages of water and ammonia are nearly equal.

Thermal desorption spectra for both water and ammonia are shown in Fig. 2 for coadsorption of water on the ammonia-covered surface. The data are grouped according to ammonia precoverage. Panel (a) shows ammonia

coverages slightly less than or equal to the completed chemisorbed state; panel (b) shows cases of slight partial filling of the second layer adsorption state; and panels (c) and (d) show, respectively, extensive and complete filling of the second layer state. The desorption characteristics of either species are largely unaffected by the other at the lowest coverages of ammonia and water studied (a1). As the water to ammonia ratio approaches unity in panel (a) a high temperature tail appears on the water desorption peak, indicating some stabilization by coadsorbed ammonia, whereas ammonia desorption remains largely unaffected by water. At the lowest water coverage in panel (b), desorption of either species is unaffected by the other, while at higher water coverages both water and ammonia desorption curves change. The water desorption peak adopts a high temperature tail (b2), and the component of ammonia desorption ascribed to the second layer peak at 130 K shifts to higher temperature with increasing water content (b2 and b3). The tendency for each species to shift the desorption of the other to higher temperatures is also exhibited for the high ammonia coverages of panels (c) and (d). The water desorption peak keeps its high temperature tail, whereas higher coverages of water (c2 and d2) manage to shift the bulk of the second layer ammonia peak to higher temperature.

Fig. 3 shows the coadsorption behavior when water is adsorbed first. Subsequent adsorption of ammonia has little effect on water desorption, and no high temperature tail appears on the water desorption peak, in contrast to the case for ammonia adsorbed first. Again, small coverages of each species desorb independently of the other as seen in curve (b). Curves (c) and (d) show that ammonia desorbs at both lower and higher temperatures than that of water, whereas some ammonia desorbs concurrently with water as seen by

the overlapping ammonia and water desorption peaks.

Vibrational spectra of ammonia in the saturated, chemisorbed state are shown as a function of water post-coverage in Fig. 4. The adsorption systems for these spectra were the same as those of Fig. 2, panel (a). The vibrational spectrum of Fig. 4a for adsorbed ammonia with just a trace of water shows the N–H stretching modes ν_1 and ν_3 in a broad peak centered at 3315 cm^{-1}, the asymmetric H–N–H deformation ν_4 (analogous to the H–O–H scissor mode) at approximately 1600 cm^{-1}, the symmetric NH_3 deformation ν_2 (umbrella mode) at 1030 cm^{-1}, and the Ag–N stretch of chemisorbed NH_3 at at 395 cm^{-1}. This last assignment is taken from energy loss results of ammonia on Ag(311) [11] in which the low frequency mode of the chemisorbed state was assigned to the Ag–N stretch, as opposed to ammonia librations, which also occur at this energy.

The other loss features are essentially identical with solid ammonia as can be seen in Table 1, which compares the energy loss peaks of selected spectra along with the main infrared transitions measured for solid ammonia and ammonia monohydrate [20-22]. Note also in Table 1, that the only ways ammonia and water can be distinguished to within the resolution of electron energy loss spectroscopy is through the ν_2 (umbrella) mode for ammonia at 1060 cm^{-1} and through the different librational energies of 650–800 cm^{-1} for water and 360–400 cm^{-1} for ammonia. Increasing the water content in the adlayer, Fig. 4b, causes relatively little change in the spectrum, but upon reaching a nearly 1:1 ratio of water to ammonia molecules, Fig. 4c, the presence of water is clearly indicated by the new librational peak at 650 cm^{-1}. (The apparent absence of a peak near 1600 cm^{-1} and the very weak feature for the N–H/O–H stretching region at 3320 cm^{-1} are consequences of

spectrometer detuning at these higher energy losses.)

Similar energy loss spectra of coadsorbed ammonia with water, except for water being deposited first, are shown in Fig. 5. Curve (a) shows the spectrum for pure water on Ag(110), which agrees with previous measurements [2]. It also illustrates the problem of spectrometer detuning in that, although water is obviously present, the scissor mode at 1590 cm^{-1} is barely visible and the O–H stretching modes not at all. Upon addition of a small amount of ammonia, to obtain a molar ratio of water to ammonia of 2.4, both species coexist on the surface as seen by the presence of both the water librational mode at 695 cm^{-1} and the ammonia umbrella mode at 1055 cm^{-1}. The N–H/O–H stretching peak at 3445 cm^{-1} was obtained after retuning the spectrometer. A further increase in the ammonia coverage, to obtain a molar ratio of 0.5, causes a disappearance of the water librational band in curve (c), but with still more ammonia, to obtain a molar ratio of 0.34, a new librational band appears at 525 cm^{-1} in curve (d). The other peaks in the spectrum, at 1035, 1585, and 3420 cm^{-1}, remain essentially unchanged.

Typical thermal desorption spectra for coadsorbed hydrogen fluoride and water are shown in Fig. 6. Representative curves for desorption of pure hydrogen fluoride and water, each adsorbed separately, are shown in (a). Hydrogen fluoride has two desorption peaks, the first layer peak 117 K and the multilayer peak at 111 K. Coadsorption with water shifts hydrogen fluoride desorption to significantly higher temperatures as shown in (b-e). With a molar ratio of water to hydrogen fluoride of 3, the onset of water desorption shifts from 138 to 128 K. Note that water desorbs first followed by hydrogen fluoride, which begins 139 K and has a trailing edge coincident with

the water desorption peak. For equal amounts of the two species, curve (c), the desorption spectra are essentially identical; two desorption peaks occur at 141 and 150 K. When the hydrogen fluoride content exceeds that of water, curves (d,e), hydrogen fluoride desorbs first with the final desorption of hydrogen fluoride also coincident with water desorption. With increasing hydrogen fluoride content (a-e) the single water desorption peak at 150 K develops into two peaks with the lower temperature peak at 141 K eventually becoming dominant. These spectra show some of the more complex interactions that occur with hydrogen fluoride and multilayer coverages of water. As presented previously [5], less complex interactions occur for submonolayer coverages of water.

4. DISCUSSION

We shall discuss the energy loss measurements first, since they were recorded immediately after adsorption at 110 K and thus represent the state of the as-deposited system. The thermal desorption spectra reveal a number of interesting interactions, some of which may occur during the temperature ramp, and we shall discuss these next. Finally, we will consider the hydrogen fluoride/water results and formation of the monohydrate.

4.1 Energy Loss Spectra of Coadsorbed Ammonia and Water

The energy loss spectra of Figs. 4 and 5, as well as many others not shown, reveal that coadsorbed ammonia and water is simply a mixture of the two species at 110 K on Ag(110). Other possibilities considered for this system were formation of a monohydrate or dihydrate, and ionization to NH_4^+ and OH^-. For comparison Table 1 lists the major infrared absorbances for

ammonia monohydrate; the distinguishing feature of either monohydrate or dihydrate is a transition around 800 cm^{-1} slightly less in intensity than the 1100 cm^{-1} transition depending on the crystallinity of the sample [21,22]. Librations that occur at lower energy belong to water molecules not uniquely coupled to ammonia. The absence of an energy loss peak at 800 cm^{-1} is conclusive proof that neither monohydrate nor dihydrate exists in the as-deposited layer at 110 K.

In solution at room temperature and pressure ammonia acts as a weak base and reacts with water to give NH_4^+ and OH^-. The pK_b of this reaction at standard conditions is 4.75 [33]. Vibrational transitions that would detect NH_4^+ are a degenerate N–H stretching mode at 3145 cm^{-1} and a degenerate deformation at 1400 cm^{-1} [34]. Infrared spectra of NH_2Cl and NH_4NO_3 detect the deformation mode between 1400 and 1500 cm^{-1} [21]. Deformation modes below 1500 cm^{-1} were not observed in any of our measurements, and hence, we can rule out the formation of ammonium ion. This finding agrees with previous infrared measurements of thick ammonia/water films [21,22].

While the energy loss spectra show an adlayer of mixed ammonia and water, they also reveal some unusual behavior of the librational modes. The librational mode of water, normally the most intense peak in the energy loss spectrum of water, is completely absent in Fig. 4(b), which represents a molar ratio of water to ammonia of 0.6. Since librational modes can only occur with water hydrogen bonded to other water molecules, we infer that water/water interactions are negligible in this case and that water interacts either with the silver surface or with other ammonia molecules. This behavior is consistent with the mechanism of dielectric screening (discussed in the next

section) in which water adsorbs among the chemisorbed ammonia molecules. The water librational mode appears for the higher molar ratio of Fig. 4(c), showing that water/water interactions are operative in this case.

Likewise, when ammonia is adsorbed onto a water adlayer, the librational mode for ammonia does not appear readily. For a molar ratio of 2.4 in Fig. 5(b) the water librational mode is clearly seen at 695 cm^{-1}, as is the ammonia deformation at 1055 cm^{-1}. However, there is no trace of ammonia librations, which should occur at 400 cm^{-1}. Thus, ammonia interacts with only water or the surface in this case. Ammonia/water interactions are evident as the water librational mode has shifted 30 cm^{-1} lower in energy from the case with water along, Fig. 5(a). For lower molar ratios (higher ammonia content) the librational modes of both species disappear in Fig. 5(c). The reason for this behavior is unknown, but clearly it marks a change in ammonia/water interactions. A librational mode at 525 cm^{-1} reappears in Fig. 5(d) for a still lower molar ratio. This new band is apparently unique to this particular set of coverages and represents a particular form of ammonia/water interaction. Also noteworthy is that the thermal desorption spectrum Fig. 3(d) recorded after this measurement shows the greatest amount of stabilization energy, as discussed in the next section.

4.2 Ammonia/Water Interactions

The thermal desorption spectra for ammonia and water adsorbed alone agree well with earlier studies of water on Ag(110) [2] and ammonia on Ag(110) [10], Ag(311) [11], and Au(111) [12]. Ammonia desorption spectra for all of these surfaces have the following features: a broad, high temperature

peak that saturates at low coverage; an intermediate temperature peak that also saturates; and a low temperature, nonsaturable peak due to multilayers. The high temperature peak of the chemisorbed state fills by shifting its leading edge rapidly to lower temperatures, as opposed to increasing its intensity. This behavior is indicative of repulsive lateral interactions [12,13] associated with charge transfer to the surface from ammonia as it adsorbs through the lone pair electrons of its nitrogen atom [10,11,18]. That this adsorption state saturates at the relatively low coverage of only 0.12 ML is further evidence of repulsive interactions.

To begin the discussion of ammonia and water coadsorption it is helpful to keep in mind the temperature range for desorption of the chemisorbed state of ammonia (145 to 200 K) and that for desorption of water, which begins at about 148 K and ends at varying temperatures depending on the amount of coadsorbed ammonia. To help identify chemisorbed ammonia, a dashed line has been placed at 145 K in Figs. 2 and 3; the temperature range for water desorption can be easily determined from the width of the corresponding desorption peak.

At sufficiently small coverages of each species, Fig. 2(a1), the desorption curves are unchanged from the case when each is adsorbed alone. Thus, each species adsorbs independently of the other. This may be explained by the two species adsorbing in separate phases on the surface, a result possible given the small coverages involved. Additional water has little effect on the chemisorbed ammonia layer at this coverage, but the latter does stabilize some of water for desorption at higher temperatures, Fig. 2(a2,3).

Ammonia becomes susceptible to interactions with water at coverages sufficient to populate the second layer, as seen in panels (b-d) of Fig. 2.

Increasing water content shifts the second layer component to higher desorption temperatures. In curve (b1) 20% of the ammonia desorbs in the second layer state below 145 K, yet essentially all of it desorbs above 145 K in the presence of water at molar ratios of 0.7 and above, curves (b2,3). Ammonia desorption in these cases exceeds the saturation value for the chemisorbed state (without water) by 20%, and a more pronounced peak appears concurrently with the water desorption peak (compare curves (b3) and (a1)).

Two possibilities exist to explain this effect: formation of an ammonia/water complex or dielectric screening by water. Beginning with the former, we note that, as previously discussed, energy loss measurements give no evidence for ammonia/water complexing. However, infrared studies of thick films of ammonia and water codeposited at 83 K show that the monohydrate complex only begins to form at 148 K [21]. Thus, a monohydrate could form during the thermal desorption experiment, though not extensively, as evidenced by the dissimilar water and ammonia desorption peaks for the case of near monohydrate stoichiometry, curve (b2). For comparison thermal desorption measurements easily detect the monohydrate of hydrogen fluoride, as discussed later.

Instead, we favor the latter mechanism of dielectric screening, which operates as follows. Ammonia molecules in the chemisorbed state should distribute themselves about the surface because of their repulsive interactions. Even at the saturation coverage of 0.12 ML (for ammonia), plenty of empty surface sites should remain for water to adsorb among the ammonia molecules. Acting as a dielectric, water screens the repulsive

interactions, thereby allowing either a tighter packing of ammonia or a greater number of ammonia molecules adsorbed directly to the surface. According to this mechanism, coadsorbed water increases the amount of chemisorbed ammonia that can be obtained. While this is a rather subtle case of dielectric screening, we have encountered similar and much more pronounced examples for the H_2O/Cl [6] and H_2O/F [7] coadsorption systems.

Coadsorbed water can stabilize significant quantities of ammonia at high coverages. At low molar ratios of water to ammonia the bulk of ammonia desorbs below 145 K in curves (c1) and (d1), but as the molar ratio reaches 0.4 or greater for curves (c2) and (d2), approximately 0.4 ML of ammonia desorbs above 145 K. This represents an enhancement over the saturation coverage of chemisorbed ammonia by a factor of three, but because of the high coverages of both species, it is unlikely that all of the ammonia desorbing at high temperature is chemisorbed. As no single adsorption state accurately describes every ammonia molecule adsorbed under these conditions, we choose instead the first moment of desorption to characterize the aggregate ammonia adlayer. In curve (c1), for example, the average desorption temperature (first moment) is 134 K; half of the ammonia desorbs at lower temperatures and the other half at higher temperatures. The first moment shifts from 134 to 148 K in panel (c) and from 140 to 149 K in panel (d); these are shown by the thin line segments in Fig. 2. When interpreted in terms of simple, first-order desorption (coverage independent parameters and pre-exponential factor of 10^{13} s^{-1}), these shifts may be used to estimate stabilization energies. Table 2 shows the shift of the first moment of desorption along with stabilization energy reported per mole of ammonia and per mole of added water. The stabilization energy results from hydrogen

bonding between ammonia and water molecules, possibly including formation of the monohydrate, and is relatively small on either basis. The values range from 1 to 7 kJ/mol and are substantially less than the hydrogen bond strength of 25 kJ/mol in the monohydrate [24]. These weaker interactions are consistent with ammonia and water not existing as a hydrated complex.

Reversal of the order of adsorption, water first followed by ammonia, produces some differences in the adlayer. At low coverages, curves (a) and (b) of Fig. 3, each species again adsorbs independently as seen by desorption curves identical with those of the species adsorbed alone. At higher coverages the influence of water is more pronounced. Both curves (c) and (d) in Fig. 3 show concurrent ammonia and water desorption peaks, indicating a more direct interaction between ammonia and water than is evident in the data of Fig. 2. Fig. 3(d) may be compared with panel (c) of Fig. 2 as the ammonia coverages are the same. Again, a large amount of ammonia, approximately 0.35 ML, desorbs above 145 K due to stabilization by water. This stabilization is much stronger than the cases for ammonia adsorbed first, as listed in Table 2. The first moment of desorption occurs at 155 K, shifted from 134 K, and the overall stabilization on both bases is substantially larger: 4.7 compared with 3.1 kJ/mol NH_3 and 9.4 compared with 1.4 kJ/mol H_2O. The ammonia basis is more significant here because of the equal coverage of ammonia for the two cases.

The differences in coadsorption behavior brought about by changing the adsorption sequence indicates the adlayer was not fully equilibrated in these experiments. Mixing of ammonia and water appears incomplete for both sequences, but it is more complete for the case of ammonia adsorbed on the water-covered surface, as judged by the stronger stabilization energies

reported in Table 2. Furthermore, concurrence of the ammonia and water desorption peaks is reasonably strong evidence in support of a monohydrate, forming during the temperature ramp of the desorption measurement.

The improved mixing of the two species with water adsorbed first may result from the weaker binding of water as compared with ammonia to the silver surface. Both species must be intermixed at the surface, as required by the dielectric screening mechanism. As the freshly deposited coadsorption system approaches equilibrium, displacement of preadsorbed water by ammonia at the surface is an energetically downhill process, whereas displacement of preadsorbed ammonia by water may involve an activation barrier, thereby producing a slower approach to equilibrium.

4.3 Formation of Hydrogen Fluoride Monohydrate

The case of coadsorbed hydrogen fluoride and water is a clear example of strong, direct interactions between the two species, which give rise to both ionization and formation of a monohydrate. Electron energy loss spectroscopy of this coadsorption system on Pt(111) [27] shows direct evidence for formation of H_3O^+. Although similar measurements have not been performed for Ag(110), there is little doubt that ionization also occurs. As discussed later, silver exhibits very little unique surface chemistry with this system and so little deviation is expected from the results for HF/H_2O multilayers on Pt(111).

. On Ag(110) the hydrogen fluoride/water coadsorption system forms an adlayer azeotrope, so identified by the tendency of the mixed adlayer to desorb at higher temperatures than either species adsorbed separately [5].

The shift in hydrogen fluoride desorption upon addition of water is dramatic, as seen in Fig. 6(a,b), whereas the shift in water desorption is only slight and not visible in this particular figure. By analogy with azeotropes in typical binary solutions, desorption of the two species occurs at constant composition. This is illustrated in Fig. 6(c) by the overlapping thermal desorption spectra for a 1:1 ratio of water to hydrogen fluoride, which represents the monohydrate $HF \cdot H_2O$. The strong conformity of the two desorption curves to each other is a hallmark of strong, direct interactions between the two species. Such conformity is not evenly remotely apparent in the ammonia/water desorption results.

A consideration of the thermodynamic aspects of Fig. 6 allows the analogy with binary solutions to be taken still further. One of the colligative properties of solutions is elevation of the boiling point due to mixing. In terms of adsorption in vacuum at low temperatures, this property becomes elevation of the sublimation point. To measure this property accurately, one must provide for reversibility; namely, the system must be set up such that sublimation (desorption) and condensation (adsorption) occur at equal rates with no net change. Normally, thermal desorption measurements are intended to be irreversible, with no readsorption of species allowed. We may, however, identify a reversible state with equal rates of adsorption and desorption that is represented by one point on the thermal desorption spectrum. This occurs at the onset of desorption of the first species from the surface. In the absence of preferential binding to the surface, as occurs for water on Ag(110), the onset of thermal desorption will be the temperature at which the vapor pressure of the adsorbate equals the partial pressure of that species in the vacuum chamber. At the onset of thermal desorption, then, the

rates of adsorption and desorption will be equal, but any increase in temperature will result in net desorption and displacement away from adsorbate/vapor equilibrium.

The temperature of the onset of thermal desorption thus serves as a measure of the sublimation point of the coadsorbate. Note in Fig. 6 that the species of greater coverage desorbs first. This behavior resembles binary solutions at their bubble point, and in fact, we may plot the onset of thermal desorption as a function of mole fraction of hydrogen fluoride x_{HF} to form curve analogous to a bubble-point curve. This is shown in Fig. 7. The filled points represent the onset of hydrogen fluoride desorption and the open circles water desorption. The so-called bubble-point curve (heavy line) shows the onset of thermal desorption as a function of composition. By analogy, we may also estimate a "dew-point" curve (thin line) from the composition of desorbing gas. The dew-point curve is related to the bubble-point curve by horizontal tie lines. For example, in Fig. 6(d) the onset of thermal desorption of essentially pure hydrogen fluoride occurs at 109 K. As desorption proceeds the adlayer becomes more dilute in hydrogen fluoride and desorbing water appears at 132 K. A horizontal tie line from this point determines where the dew point curve begins to deviate from the pure HF line ($x_{HF} = 1$). The rest of the dew-point curve, which must meet the bubble-point curve at the azeotrope, can be easily filled in.

The points in Fig. 7 fall on a common curve and represent data for total surface coverages ranging from 0.3 to 10 ML; no differences exist between submonolayer and multilayer coverages. Hence, the silver surface is chemically inert here and serves only as a thermostat. This verifies the

assumption of no preferential binding to the surface and so the analogy between onset of thermal desorption and sublimation temperature is valid. By virtue of the inert surface, only the relative coverages of hydrogen fluoride and water are important here, and we may thus use mole fraction of hydrogen fluoride x_{HF} as the independent variable.

5. CONCLUSIONS

The ammonia/water and hydrogen fluoride/water coadsorption systems illustrate cases of weak and strong interactions with water. Whereas ammonia exhibits reasonably strong preferential adsorption on Ag(110), it engages in relatively weak interactions with water. Conversely, hydrogen fluoride interacts only weakly with Ag(110), but quite strongly with water to form a monohydrate.

Ammonia and water simply coexist when coadsorbed at 110 K and neither ionize nor form distinct hydrated complexes. The chemisorbed ammonia state saturates at 0.12 ML in the absence of water and has lateral repulsive interactions. Coadsorbed water can increase the amount of chemisorbed ammonia by acting as a dielectric and screening the ammonia/ammonia repulsive interactions. Water stabilizes high coverages of ammonia and raises the average (first moment) desorption temperature by 9 to 21 K. The stabilization energies are on the order of 2 – 5 kJ/mol NH_3 and 1–9 kJ/mol H_2O. Ammonia/water adlayers formed sequentially do not reach equilibrium, although mixing is enhanced if ammonia is adsorbed on a water precovered surface.

Hydrogen fluoride and water, adsorbed separately, have distinctly different temperatures of 117 and 150 K, yet the thermal desorption curves

completely overlap for a 1:1 mixture of the species, indicative of the monohydrate $HF \cdot H_2O$. This system exhibits many analogies with typical binary solutions. An adlayer azeotrope can be identified and the onset of thermal desorption can be used to construct analogous bubble-point and dew-point curves.

ACKNOWLEDGEMENTS

This work has benefited from many stimulating discussions with Fred Wagner. We gratefully acknowledge support of this work by the Office of Naval Research.

REFERENCES

1. K. Franaszczuk, E. Herrero, P. Zelenay, A. Wieckowski, J. Wang, and R. Masel, *J. Phys. Chem.*, 1992, **96**, 8509.
2. E. M. Stuve, R. J. Madix and B. A. Sexton, *Surface Sci.*, 1981, **111**, 11.
3. K. Bange, T. E. Madey, J.–K. Sass and E. M. Stuve, *Surface Sci.*, 1987, **183**, 334.
4. P. A. Thiel and T. E. Madey, *Surface Sci. Rep.*, 1987, **7**, 211.
5. E. M. Stuve and N. Kishakevariam, *J. Vac. Sci. Technol. A*, 1993, **11**, 2217.
6. N. Kizhakevariam, E. M. Stuve, and R. Döhl-Oelze, *J. Chem. Phys.*, 1991, **94**, 670.
7. A. Krasnopoler, A. L. Johnson, and E. M. Stuve, *Surface Sci.*, 1995, **328**, 186.
8. A. Krasnopoler and E. M. Stuve, *Surface Sci.*, 1994, **303**, 355.
9. A. Krasnopoler and E. M. Stuve, *J. Vac. Sci. Tech. A*, 1995, **13**, 1681.

10. J. L. Gland, B. A. Sexton and G. E. Mitchell, *Surface Sci.*, 1982, **115**, 623.
11. S. T. Ceyer and J. T. Yates, Jr., *Surface Sci.*, 1985, **155**, 584.
12. B. D. Kay, K. R. Lykke, J. R. Creighton, and S. J. Ward, *J. Chem. Phys.*, 1989, **91**, 5120.
13. K. J. Wu and S. D. Kevan, *J. Chem. Phys.*, 1991, **95**, 5355.
14. T. Hertel, M. Wolf, and G. Ertl, *J. Chem. Phys.*, 1995, **102**, 3414.
15. P. R. Davies, M. W. Roberts, N. Shukla, and D. J. Vincent, *Surface Sci.*, 1995, **325**, 50.
16. H. E. Dastoor, P. Gardner, and D. A. King, *Surface Sci.*, 1993, **289**, 279.
17. G. B. Fisher, *Chem. Phys. Lett.*, 1981, **79**, 452.
18. J. A. Rodriguez, W. K. Kuhn, C. M. Truong, and D. W. Goodman, *Surface Sci.*, 1992, **271**, 333.
19. C. Benndorf and T. E. Madey, *Surface Sci.*, 1983, **135**, 164.
20. F. P. Reding and D. F. Hornig, *J. Chem. Phys.*, 1951, **19**, 594; 1955, **23**, 1053.
21. T. Huston, I. C. Hisatsune, and J. Heicklen, *Can. J. Chem.*, 1983, **61**, 2077.
22. J. E. Berite and M. R. Shehata, *J. Chem. Phys.*, 1985, **83**, 1449.
23. A. Engdahl and B. Nelander, *J.Chem. Phys.*, 1989, **91**, 6604.
24. P.-O. Åstrand, G. Karlström, A. Engdahl, and B. Nelander, *J. Chem. Phys.*,1995, **102**, 3534.
25. R. Fournier, *J. Chem. Phys.*, 1995, **102**, 5396.
26. C. E. Dykstra and L. Andrews, *J. Chem. Phys.*, 1990, **90**, 6043.
27. F. T. Wagner and T. E. Moylan, *Surface Sci.*, 1987, **182**, 125.
28. R. Döhl-Oelze, C. C. Brown, S. Stark, and E. M. Stuve, *Surface Sci.*,

1989, **210**, 339.

29. N. Kizhakevariam and E. M. Stuve, *Surface Sci.*, 1992, **275**, 223.
30. A. C. Liu and C. M. Friend, *Rev. Sci. Instrum.*, 1986, **57**, 1519.
31. J. F. O'Hanlon, *A User's Guide to Vacuum Technology*, Wiley, New York, 1989.
32. *Crystal Data Determinative Tables*, 3rd ed., Vol. II, (ed.) J. D. H. Donnay and H. M. Ondik, U. S. Dept. of Commerce NSRDS, 1973, p. C-93.
33. *CRC Handbook of Chemistry and Physics*, 66th ed., ed. R. C. Weast, CRC Press, Boco Raton, Florida, 1985, p. D-161.
34. K. Nakamoto, *Infrared and Raman Spectra of Inorganic and Coordination Compounds*, Wiley, New York, 1986.

Table 1. Vibrational modes for ammonia and water adsorbed alone and coadsorbed on Ag(110) in comparison with those of solid ammonia and ammonia monohydrate.

Mode	NH_3 solid [21,22]	NH_3 ads. Fig. 4a	H_2O/NH_3 ads. Fig. 4c	$NH_3 \cdot H_2O$ solid [21,22]	NH_3/H_2O ads. Fig. 5d	H_2O ads. [2]
ν_1, ν_3 [a]	3380	3315	3320	3380	3420	3410
ν_{OH} [a]	3290			3220		
ν_4 [b]	1650	~1600		1630	1585	1660
ν_2 [c]	1060	1030	1025	1100	1035	
$\rho(H_2O)$ [d]			650	800	525	740
$\rho(NH_3)$ [d]	360			400		
$\nu_{Ag\text{-}N}$ [e]		395				
τ [f]					220	200

[a] N–H and O–H stretching modes

[b] Asymmetric H–N–H bending modes; H–O–H scissor mode

[c] Symmetric NH_3 deformation (umbrella mode)

[d] Librational modes (frustrated rotations)

[e] Ag–N stretching mode

[f] Frustrated translational modes

Table 2. Shifts in the first moment of ammonia desorption $\Delta\langle T\rangle$ from Figs. 2(c,d) and 3(d) and corresponding stabilization energies based on ammonia ΔE_A or added water ΔE_W.

System	θ_A / ML	$\Delta\theta_W$ / ML	$\Delta\langle T\rangle$ / K	ΔE_A / kJ mol^{-1}	ΔE_W / kJ mol^{-1}
H_2O/NH_3	0.6	1.3	14	3.1	1.2
H_2O/NH_3	1.0	0.3	9	2.2	7.3
NH_3/H_2O	0.6	0.3	21	4.7	9.4

FIGURE CAPTIONS

Figure 1: Thermal desorption spectra of water and ammonia, each adsorbed alone, as a function of coverage on Ag(110). The adsorption temperature was 110 K. The inset shows the ammonia coverage, as determined by the area under the desorption peaks, as a function of exposure. The exposure values were determined directly from an uncorrected ion gauge and do not reflect the enhancement factor due to the microcapillary array used for dosing.

Figure 2: Thermal desorption spectra of water (thin lines) and ammonia (heavy lines) for water coadsorbed with ammonia (ammonia deposited first) as a function of coverage. Each panel shows a fixed coverage of ammonia: (a) 0.12, (b) 0.14, (c) 0.7, and (d) 1.1 ML. The molar ratios of water to ammonia were (a1) 0.2, (a2) 0.6, and (a3) 0.9; (b1) 0, (b2) 0.7, and (b3) 5.1; (c1) 0 and (c2) 1.8; and (d1) 0.2 and (d2) 0.4. The magnification indicated for each panel applies to all curves in that panel except as noted.

Figure 3: Thermal desorption spectra of water (thin lines) and ammonia (heavy lines) for ammonia coadsorbed with water (water deposited first) as a function of coverage. The water precoverage was (a) 0.15, (b) 0.13, (c) 0.12, and (d) 0.30 ML. The molar ratios of water to ammonia were (a) infinite, (b) 2.4, (c) 0.5, and (d) 0.34.

Figure 4: Electron energy loss spectra for water coadsorbed with 0.12 ML of ammonia (ammonia deposited first). Spectra (a), (b), and (c) were recorded just prior to the thermal desorption measurements (a1), (a2), and (a3), respectively, shown in Fig. 2. The molar ratios of

water to ammonia were (a) 0.2, (b) 0.6, and (c) 0.9.

Figure 5: Electron energy loss spectra for ammonia coadsorbed with water (water deposited first). Each spectrum was recorded just prior to the corresponding thermal desorption measurement of Fig. 3. The water precoverage was (a) 0.15, (b) 0.13, (c) 0.12, and (d) 0.30 ML. The molar ratios of water to ammonia were (a) infinite, (b) 2.4, (c) 0.5, and (d) 0.34.

Figure 6: Thermal desorption spectra of (a) 1.9 ML of hydrogen fluoride and 0.3 ML of water adsorbed separately and (b-e) hydrogen fluoride coadsorbed with 1.5 ML of water (water adsorbed first) on Ag(110) at 90 K. The coverages of hydrogen fluoride were (b) 0.5, (c) 1.5, (d) 3.4, and (e) 5.1 ML. The heavy lines show hydrogen fluoride desorption, multiplied by a factor of four relative to the water spectra of (b-e), and the thin lines show water desorption. Dashed lines indicate overlap of the two curves.

Figure 7: Onset of thermal desorption T_o as a function of mole fraction hydrogen fluoride x_{HF} for coadsorbed HF and H_2O on Ag(110). The heavy line represents the bubble-point curve and the thin line the dew-point curve. See text for further details.

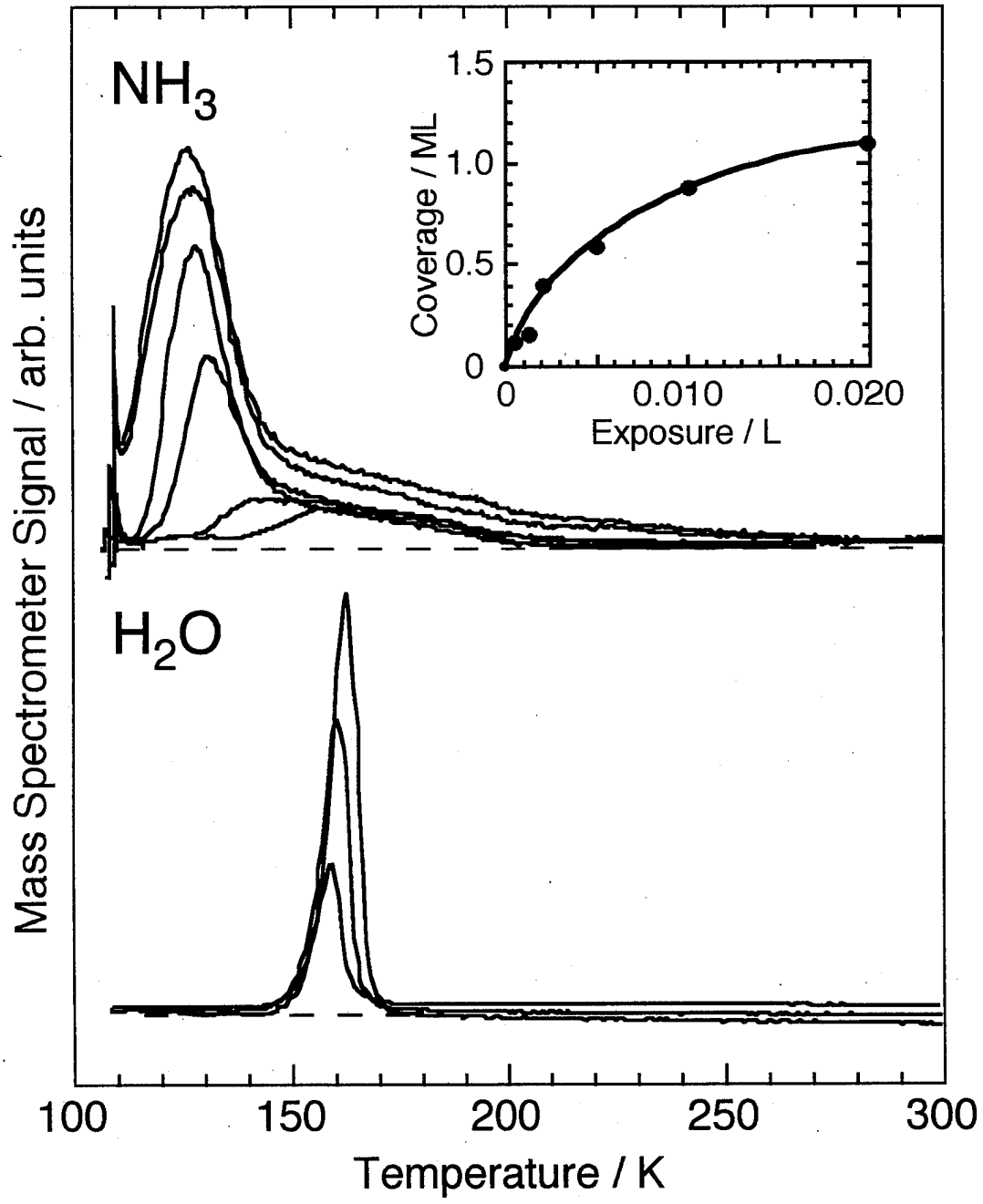

Fig. 1, Krasnopoler, et al.

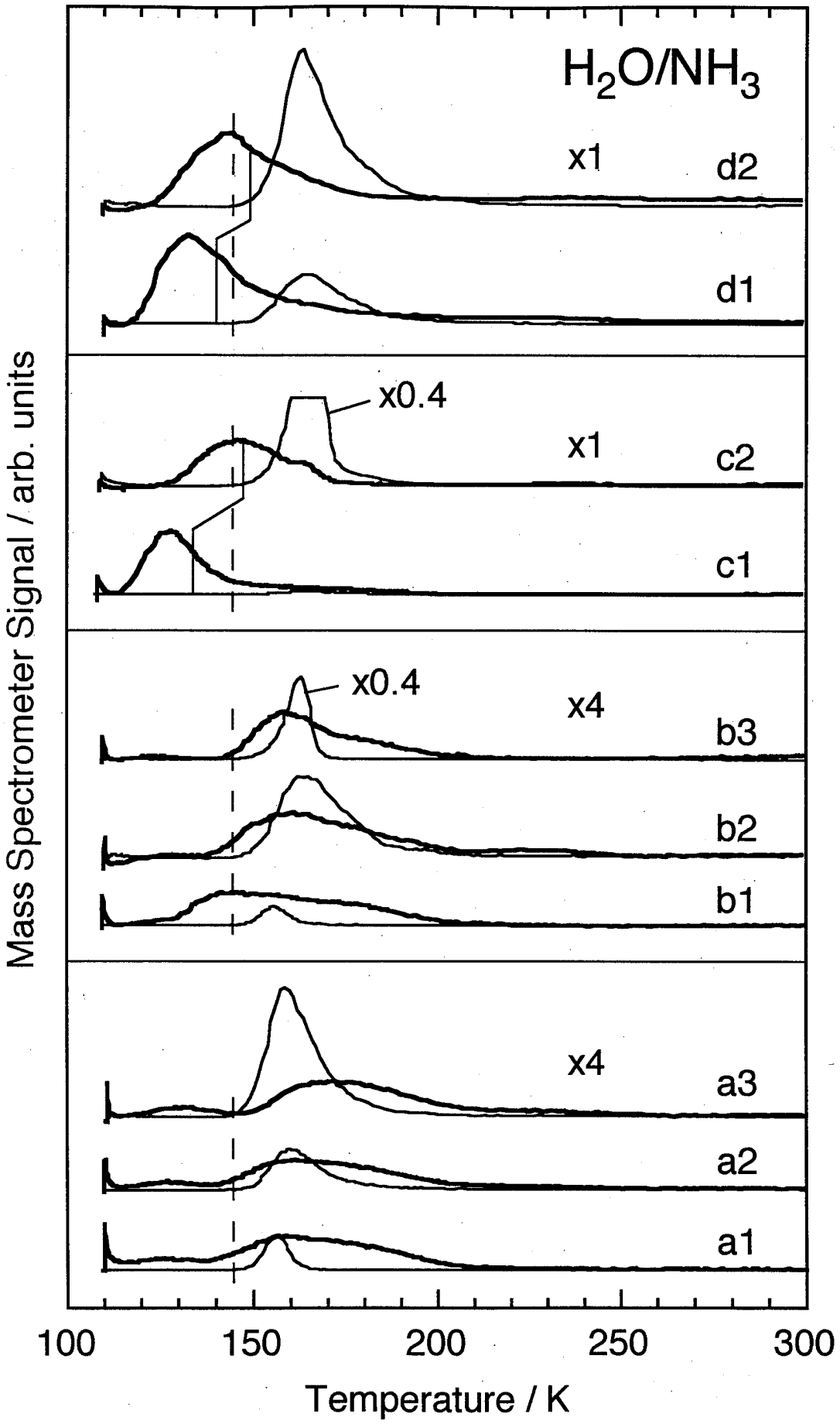

Fig. 2, Krasnopoler, et al.

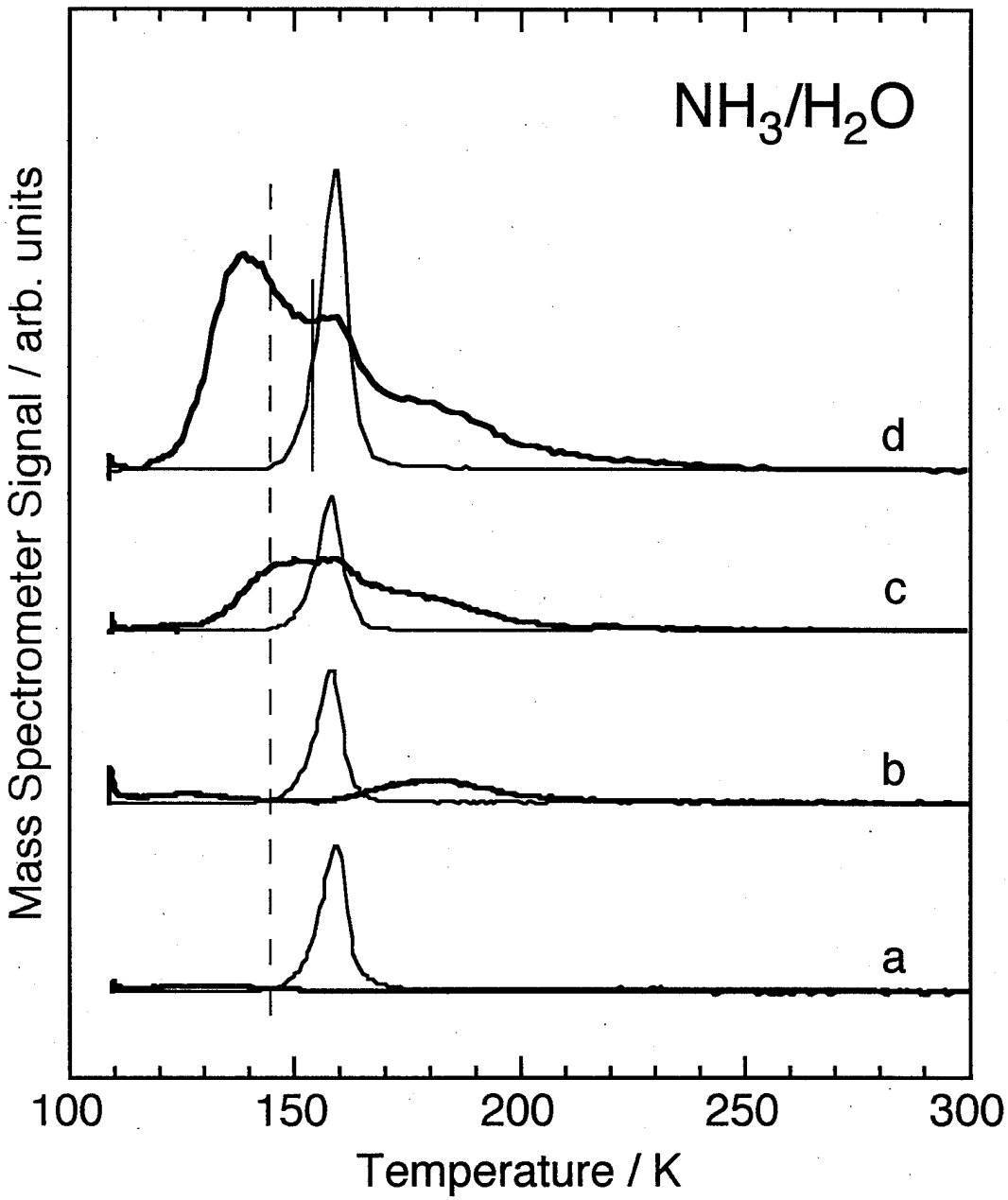

Fig. 3a, Krasnopoler, et al.

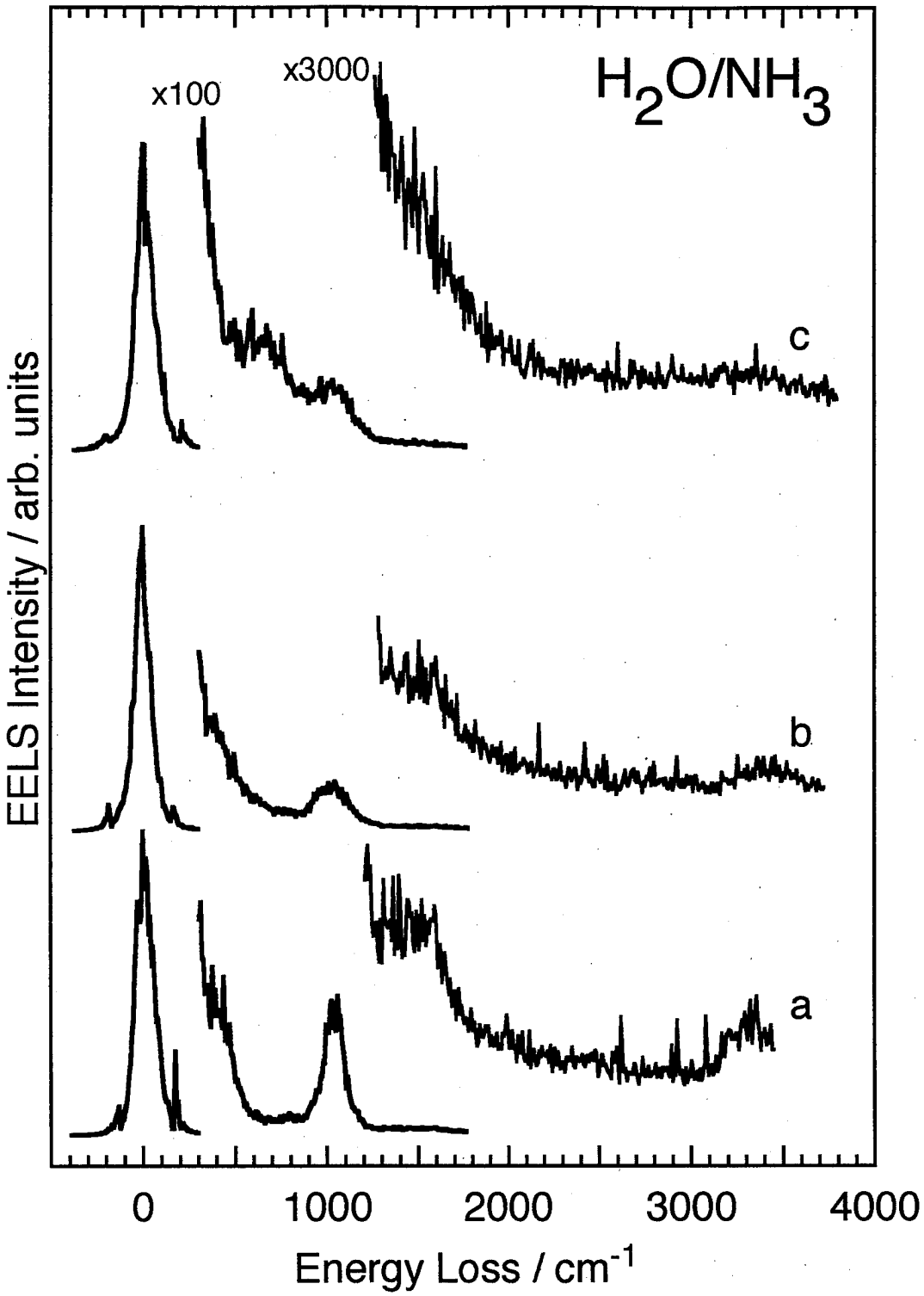

Fig. 4, Krasnopoler, et al.

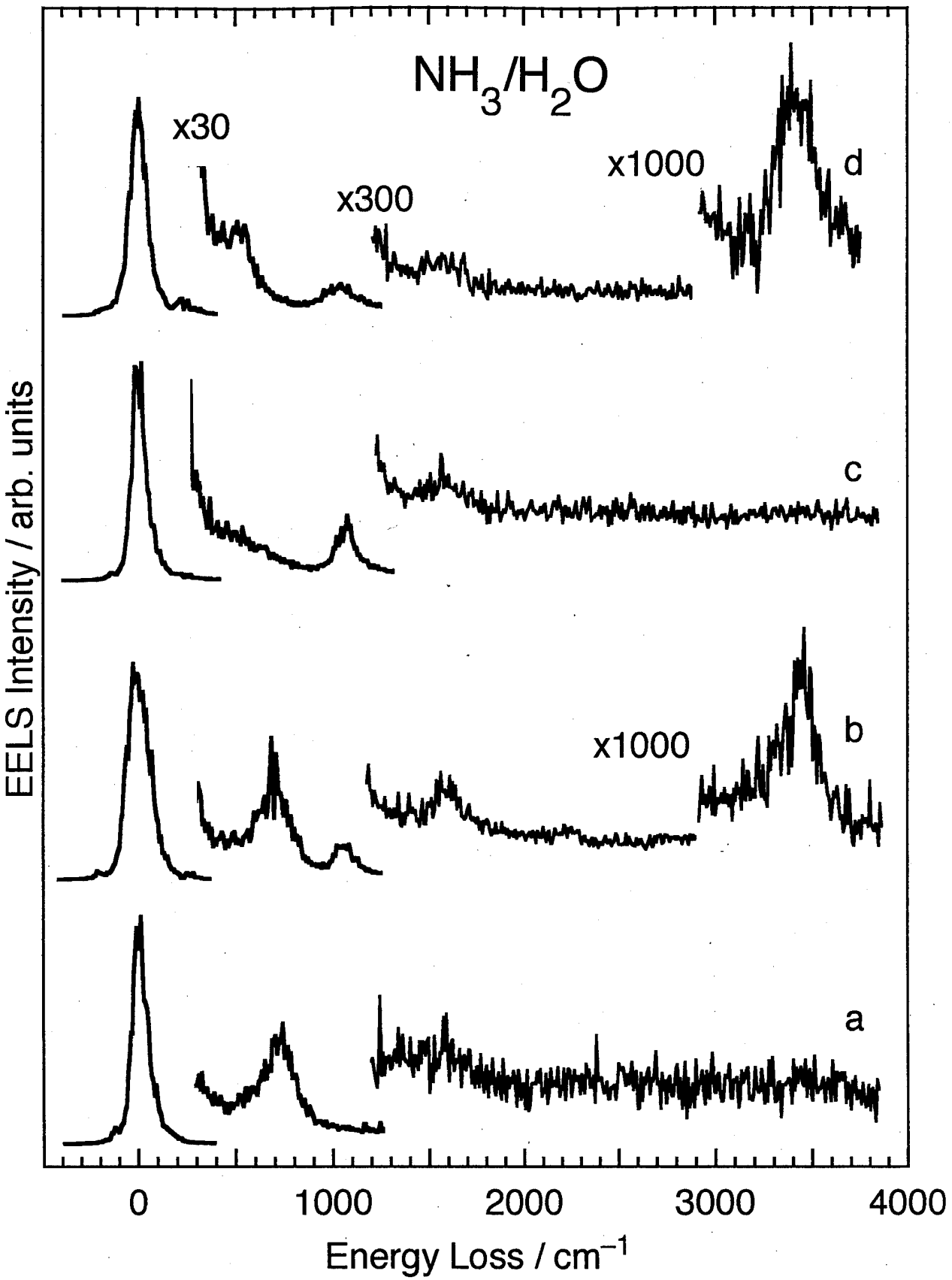

Fig. 5, Krasnoperla, et al.

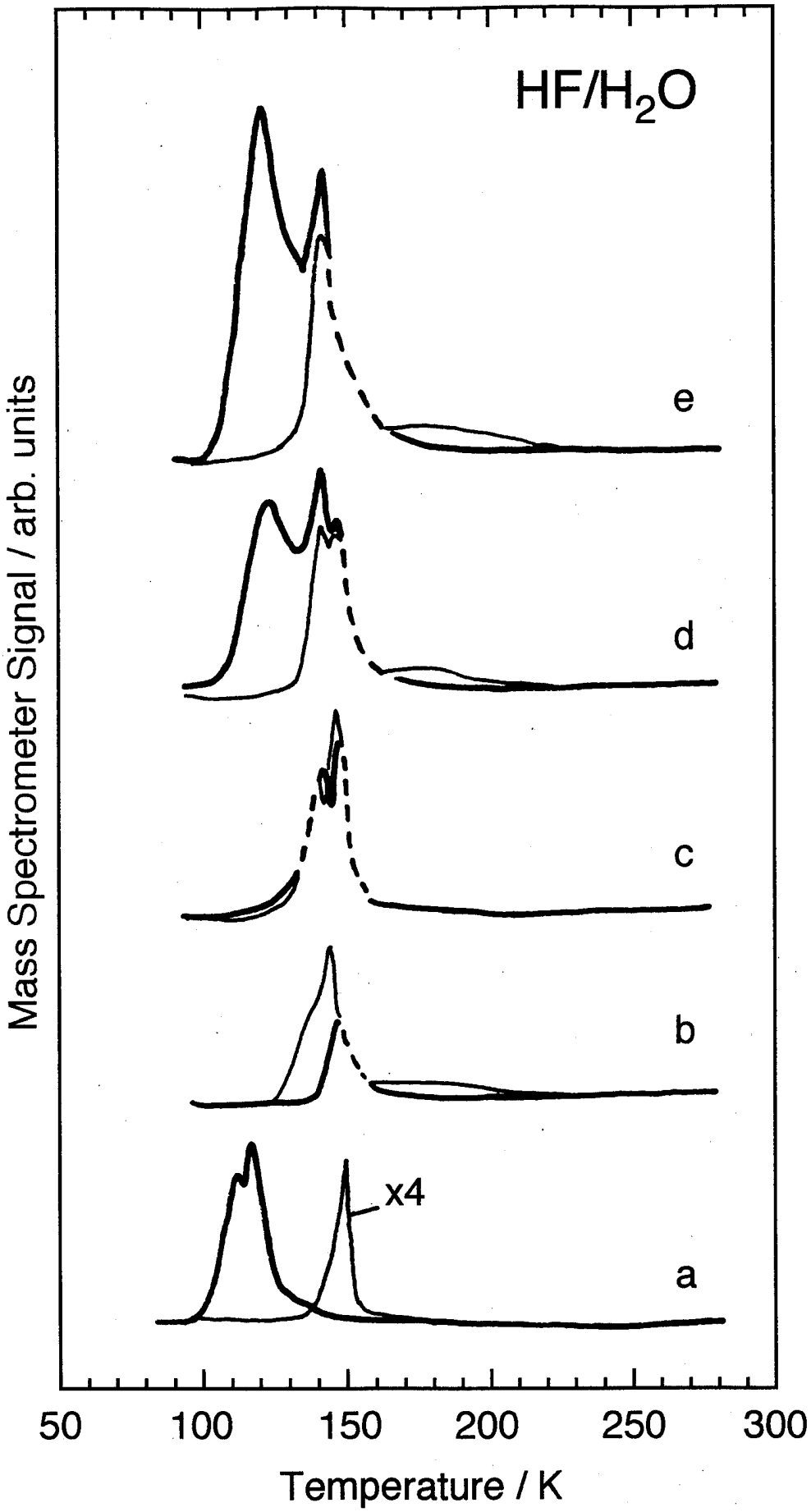

Fig. 6, Krasnoperov, et al.

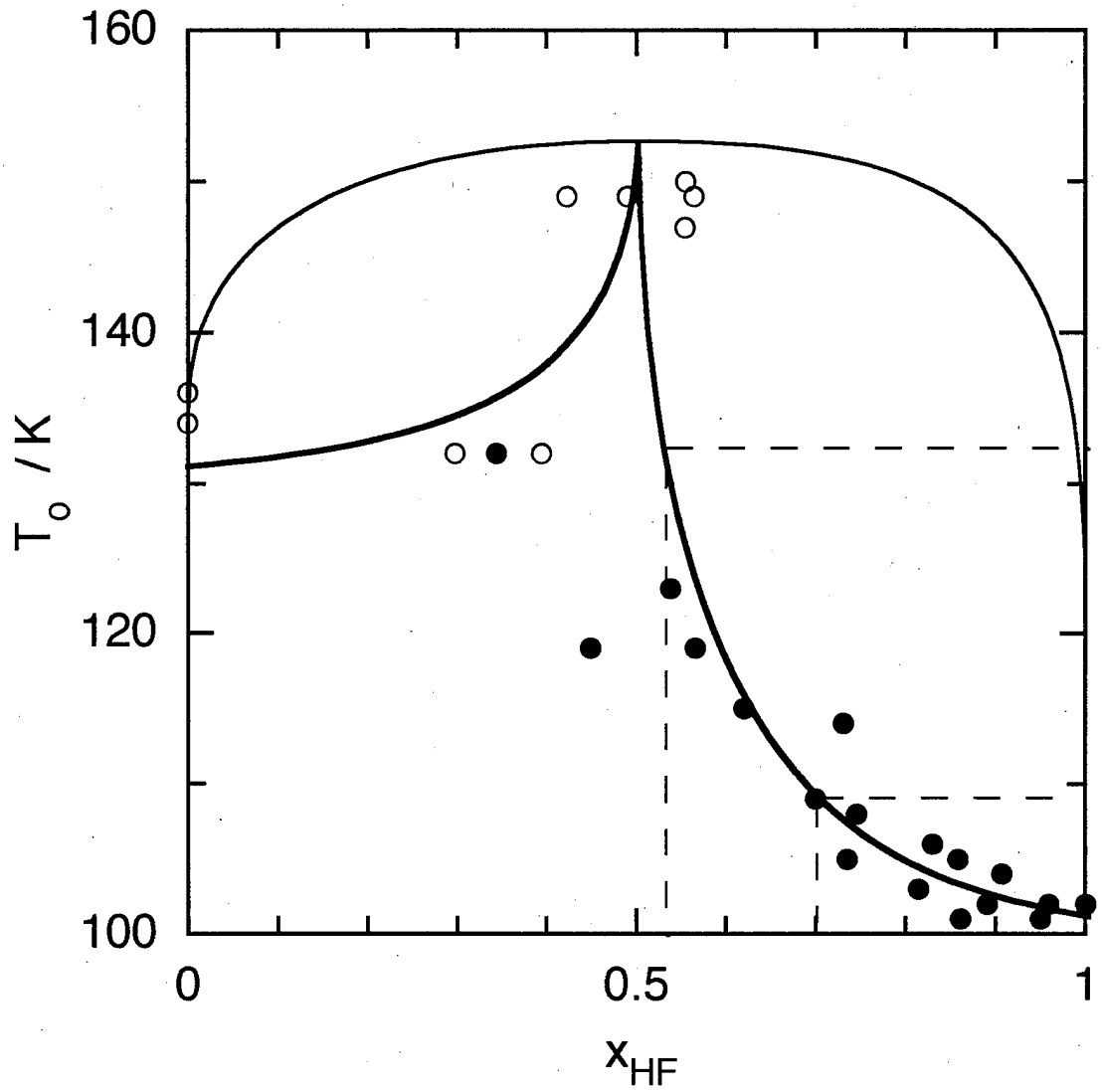

Fig 7, Krasnopoler, et al.